Published in final edited form as:
J Comput Chem. 2008 January 15; 29(1): 17–23. doi:10.1002/jcc.20625.

Molecular Mechanics Parameters for the FapydG DNA Lesion

Kun Song[1], **Viktor Hornak**[2], **Carlos de los Santos**[3], **Arthur P. Grollman**[3], and **Carlos Simmerling**[1,4]

[1]Department of Chemistry, Stony Brook University, Stony Brook, New York 11794-3400

[2]Center for Structural Biology, Stony Brook University, Stony Brook, New York 11794-3400

[3]Department of Pharmacological Sciences, Stony Brook University, Stony Brook, New York 11794-3400

[4]Computational Science Center, Brookhaven National Laboratory, Upton, New York 11973

Abstract

FapydG is a common oxidative DNA lesion involving opening of the imidazole ring. It shares the same precursor as 8-oxodG and can be excised by the same enzymes as 8-oxodG. However, the loss of the aromatic imidazole in FapydG results in a reduction of the double bond character between C5 and N7, with an accompanying increase in conformational flexibility. Experimental characterization of FapydG is hampered by high reactivity, and thus it is desirable to investigate structural details through computer simulation. We show that the existing Amber force field parameters for FapydG do not reproduce X-ray structural data. We employed quantum mechanics energy profile calculations to derive new molecular mechanics parameters for the rotation of the dihedral angles in the eximidazole moiety. Using these parameters, all-atom simulations in explicit water reproduce the nonplanar conformation of cFapydG in the crystal structure of the complex with L. lactis glycosylase Fpg. We note that the nonplanar structure is stabilized by an acidic residue that is not present in most Fpg sequences. Simulations of the E->S mutant, as present in E. coli, resulted in a more planar conformation, suggesting that the highly nonplanar form observed in the crystal structure may not have direct biological relevance for FapydG.

Introduction

Cellular DNA is constantly facing oxidative stress from both exogenous and endogenous resources, which damages DNA by creating oxidative lesions. Failure to repair these lesions can lead to aging related diseases, including cancer.[1,2] Among these lesions, 8-oxo-guanine (8-oxodG)[3] is one of the most common forms.[4] Failure to repair the damaged base can cause G:C to T:A transversion.[5] 2,6-diamino-4-hydroxy-5-formamidopyrimidine (FapydG), another common form of oxidative lesion, shares the same precursor as 8-oxodG (see Fig. 1).[6] Both DNA lesions can be excised by DNA glycolases in prokaryotes and eukaryotes. [7] Because of the increased conformational freedom due to the imidazole ring rupture, it is important to compare the mechanisms of recognition of FapydG and 8-oxodG by the corresponding glycosylase enzymes. However, due to the opened imidazole ring, FapydG tends to anomerize and decompose under conditions required for *in vitro* DNA synthesis, which will reduce the purity of the synthesized oligonucleotides containing this lesion. This increases the difficulty in studying FapydG. Therefore, unlike the many studies done on the

recognition of 8-oxodG, relatively little structural information has been obtained about how FapydG is recognized by DNA repair enzymes.

Two types of FapydG analogs in which the ribose is replaced by a pentane ring (*c*FapydG), β-C-FapydG[8–11] and carbocyclic FapydG,[12–14] have been often used as a substitute for FapydG, since they exhibit increased stability. However, caution must be used when using *c*FapydG data to gain insight into unmodified FapydG behavior. Molecular mechanics studies can study FapydG directly, and can also provide insight into any differences between *c*FapydG and FapydG, providing a useful framework to interpret *c*FapydG experimental data. This type of simulation depends critically on the accuracy of the molecular mechanics parameters employed. Since FapydG is a nonstandard nucleotide, the parameters are not as mature and well validated as those for standard DNA and RNA systems. The major goal of this study is to develop and validate the parameters used in the simulations of FapydG containing systems. The resulting parameters will be used in future simulation studies of the dynamic aspects of FapydG recognition.

Coste et al. solved the crystal structure of Fpg from *Lactococcus lactis* (L*l*Fpg) bound to a cFapydG containing DNA.[12] Although both FapydG and 8OG are excised by Fpg, the *c*FapydG lesion is observed to adopt the *anti*-conformation in the Fpg active site, while 8OG is observed in the syn conformation in the active site of B. *st.* Fpg.[15] One interesting feature is that *c*FapydG is highly nonplanar (the dihedral angle C4—C5—N7—C8 is −103°). This conformation is stabilized by waterbridged interactions between the O8 of *c*FapydG and side chain hydroxyl of Tyr238, and between the N7 of *c*FapydG and the carbonyl O of Met75. Tyr238 also forms a hydrogen bond with the *c*FapydG phosphate (Fig. S1).

Computational studies of the recognition of FapydG by the E. *coli* repair enzyme Fpg have been reported by Perlow- Poehnelt et al.[16] The authors carried out 2 ns explicit solvent all-atom MD simulation using the Amber ff99 force field[17] from two different starting structures; simulations initiated with *anti* FapydG adopted the water bridged interaction between Met73 (Met75 in *Ll* Fpg) and FapydG as seen in the crystal structure. However, the resulting simulation model of the interaction of *E. coli* FapydG with Fpg is not consistent with the X-ray structure of *c*FapydG bound to *L. lactis* Fpg. One significant difference is the dihedral angles for C4—C5—N7—C8, which has values of −103° and 164°in the crystal structure and previous simulations, respectively. Another difference is in the amide conformation for C5—N7—C8—O8, which is *cis* in the crystal structure and trans in the simulation model (see Fig. 2). It should be pointed out that the sequences of *L. lactis* and *E. coli* Fpg differ, e.g., position 77 is Glu in *Ll* and Ser in *E. coli*. We previously reported that the presence of the acidic residue at this position can affect the conformation of a bound lesion.[18] It is possible that the difference between the Perlow-Poehnelt et al. study and the X-ray structure is due to this sequence difference. It could also arise from differences between FapydG and *c*FapydG.

Although Perlow-Poehnelt et al. generated new partial atomic charges for the FapydG lesion, the dihedral parameters for bond rotation profiles were adopted from the Amber ff99 force field[17] without modification. Because of the opening of the imidazole ring, FapydG has different resonance structures from dG, with loss of aromaticity for the eximidazole ring

in FapydG. This could be expected to dramatically change the energy profile for rotation about bonds that no longer have significant double bond character, such as C4—C5—N7—C8, suggesting that the dihedral parameters for dG may not appropriate for FapydG. In this study we used *ab initio* calculations to calculate the energy profile for the rotation of the dihedral angles C4—C5—N7—C8 and C5—N7—C8—O8 (see Fig. 2). The results show that the former has a significantly reduced rotational barrier as compared to what was defined in ff94/ff99, and the latter is essentially unchanged with significant double bond character. New molecular mechanics parameters were obtained through fitting to these *ab initio* energy profiles.

We performed simulations of a DNA duplex containing FapydG, in complex with Fpg from *Bacillus stearothermophilus* (*B.st.* Fpg). The initial model was based on the crystal structure of the complex, with the exception that the experimental structure employed *c*FapydG (PDB ID 1XC8[12]). Using partial charges derived for FapydG along with bond, angle, and dihedral parameters obtained from standard ff99, we obtain a planar *antitrans*-FapydG that is not in agreement with the nonplanar *antitrans*- *c*FapydG crystal structure. In contrast, when the simulations are repeated using the optimized dihedral parameters, the resulting structure is in close agreement with the experimental structural data. This suggests that the crystal structure of the complex containing *c*FapydG is a reasonable model for the interaction of Fpg with FapydG. However, in simulations in which the Glu77 was changed to the more frequently occurring Ser (as found in *E. coli*), we obtained a more planar conformation even when the new parameters were employed. This observation is consistent with previous simulation results that employed *E. coli* Fpg.[16] The results demonstrate that the standard Amber parameters, which give planar FapydG conformations for both Fpg sequences, are unable to reproduce the sensitivity of the lesion to the presence of the acidic residue. Since this acidic residue is not conserved, the simulation data suggest that the nonplanar conformation observed in the crystal structure may not have direct biological relevance. Overall, the results provide further evidence that simulations with the new force field parameters will be a useful component of structural studies on FapydG lesions and provide an avenue to explore possible artifacts in experiments arising from the use of *c*FapydG as a model for FapydG.

Methods

Calculation of Partial Atomic Charges

Partial atomic charges were calculated following previously published procedures[19] in order to be consistent with the ff99 force field. One dimethylphosphate (DMP) and four starting structures of the FapydG nucleoside were used. The initial nucleoside structures included *cis* and *trans* C5—N7 paired with *cis* and *trans* N7—C8 (Fig. 2). These structures were optimized using Gaussian03,[20] with Hartree-Fock calculations and the 6-31G* basis set. A two-step RESP fitting procedure[19] was carried out using the program RESP[21] in Amber.[22] Atom types were assigned by analogy. The resulting partial charges and atom type assignments are provided in Table S1.

Ab Initio Calculation of Rotational Energy Profiles

The deoxynucleoside FapydG was used to obtain rotational energy profiles. Because of the difficulty of rotating the N7—C8 amide bond, the energy profiles for the rotation of the two rotatable bonds were calculated separately for the two N7—C8 isomers. For the C5—N7 bond, snapshots were generated by performing a relaxed potential energy surface scan in 10° increments using Gaussian03 at the HF/6-31G* level, repeated for *cis* and *trans* conformations of N7—C8 (Fig. 2), resulting in 72 structures. In this calculation, structures were optimized with this dihedral angle constrained. For the N7—C8 bond, four conformations with dihedral angle C5—N7—C8—O8 of 08, 90°, 180°, and 270° were built using Schrödinger maestro and optimized using HF/6-31G*. Energy profiles were calculated using single point energies at the MP2/6-31G* level for the optimized conformations.

Generation of New Molecular Mechanics Dihedral Parameters

Molecular mechanics energy profiles were calculated using standard Amber ff99 force field without any dihedral terms for X—C5— N7—X, providing a baseline energy for calculation of the required correction terms. The process was subsequently repeated using standard and modified ff99 in order to determine the extent to which the new parameters improve the fit to the *ab initio* data.

The torsional terms were calculated using the following procedure. (1) The difference between the energy profile from the MP2 calculations described above and the MM energy without explicit dihedral term was calculated. (2) Equation (1) was used in a nonlinear least-squares fit to obtain parameters that minimize this difference. Since C5 and N7 are expected to employ sp^2 hybrid orbitals, two cosine terms with periodicities of 1 and 2 were employed.

$$\mathrm{E_{tors}}=V_1 \times (1+\cos(\phi-\gamma 1))+V_2 \times (1+\cos(2\phi-\gamma 2))$$

Equation (1). The equation used for fitting the modified torsion terms for rotation about C5—N7 and N7—C8. V_1 and V_2 are force constants, φ is the dihedral angle and γ1 and γ2 are phases.

Molecular Dynamics Simulations

To facilitate future comparisons with simulations using 8-oxoguanine, we employed the *Bacillus stearothermophilus (B. st.)* Fpg sequence that we used previously.[18] Consequently, all sequence numbering corresponds to the *B. st.* sequence. The starting structure was built based on the crystal structure of Fpg bound to DNA containing 8-oxo-guanine (PDB ID 1R2Y[15]) with the exception that the FapydG conformation was built using the *c*FapydG conformation in the crystal structure of *L. lactis* Fpg (PDB ID 1XC8[12]). The Q2 mutation used to inactivate the enzyme was reverted to wild type E2. To study the effect of the acidic residue at position 77 (*E. coli* Fpg has Ser at this position), we also performed simulations on the E77S mutant.[18] Fpg sequences from both *B. St*. and *L. lactis* have Glu at this position. The structures were minimized for 100 cycles of steepest descent and then solvated in truncated octahedron box with a minimum 6 Å buffer between the box edge and the nearest protein atom. The TIP3P model[23] was used to explicitly represent 7356 water molecules.

Following previous studies,[16,24] the N-terminal proline was modeled as neutral to mimic the stage directly before the reaction. The parameters for neutral N-terminal proline were obtained from Perlow-Poehnelt et al.[16] All molecular dynamics simulations were carried out with the SANDER module in Amber. The solvated systems were minimized and equilibrated following our previously reported studies on Fpg in complex with DNA containing 8-oxodG[18]: (i) 50 ps MD simulation with protein and DNA atoms constrained and movement allowed only for water; (ii) five 1000-step cycles of minimization, in which force constants for positional restraints on the protein and DNA atoms were gradually decreased; (iii) four cycles of 5000 steps MD simulation with decreasing restraints on protein and DNA. A final 5000 steps of MD were performed without restraints. The resulting structures were used in the production runs.

SHAKE[25] was used to constrain bonds involving hydrogen atoms. The nonbonded cutoff was 8 Å. The particle mesh Ewald method[22] was used to calculate long-range electrostatics. Constant pressure (1 atm) and temperature (300 K) were maintained by the weak coupling algorithm.[26]

Results and Discussion

Simulation Results Using the Default Amber ff99 Parameters

*c*FapydG adopts a nonplanar, *cis* conformation in the crystal structure (see Fig. 3).[12] The dihedral angle of C4—C5—N7—C8 is −103°, and the O8 of *c*FapydG interacts with Tyr238 through a water molecule. This interaction may be important for lesion recognition since O8 is absent in undamaged guanine, but is present for both the FapydG and 8OG lesions that are excised by Fpg. In contrast, FapydG structures observed in previously reported MD simulations on *E. coli* Fpg complex were more nearly planar (164° for the *anti-trans*-FapydG).[16] Our 4 ns simulation using standard Amber ff99 dihedral parameters that were initiated in the nonplanar *anti-cis*-FapydG crystal conformation spontaneously adopted a highly planar FapydG structure (Fig. 3), with a C4—C5—N7—C8 dihedral angle of (−5±14)° (uncertainty denotes the standard deviation) (Fig. 6).

Energy Profiles for C5–N7 Bond Rotation

The major reason that *c*FapydG is nonplanar in the X-ray structure is rotation about C4—C5—N7—C8 with a dihedral angle of −103°. The opened ring can reduce the partial double bond character of the C5—N7 bond, lowering the energy barrier sufficiently for a water-bridged hydrogen bond to induce the nonplanar conformation seen in the crystal structure. To test this possibility, we generated the *ab initio* energy profiles for C5—N7 bond rotation (see Methods). The results are shown in Figure 4 for the energy profiles obtained at the MP2 level as well as the profile obtained using standard ff99-based parameters.[24] The energy profiles are in poor agreement, and the difference between them varies depending on whether the neighboring N7—C8 amide is in the *syn* or *anti* conformation. We note that the energy minimum in *cis* FapydG for C4—C5—N7—C8 is a planar conformation with a dihedral value of zero, consistent with our simulation results using standard ff99 but in conflict with the nonplanar *cis* FapydG seen in the crystal structure. For *trans* FapydG, the minimum energy conformation is nonplanar, consistent with previously reported simulations

that employed *trans* FapydG. Importantly, ff99 MM energies for nonplanar conformations are substantially larger than observed in the MP2 data for both *cis* and *trans* FapydG.

To generate new torsional parameters for the C5—N7 bond, we calculated the difference between the energies from the MP2 profile and those obtained from a calculation using ff99 without any dihedral terms for C5—N7 (see Methods). New parameters were obtained through fitting to this difference function, with the resulting parameters shown in Table 1 and a comparison of the energy profiles for the original and new parameters shown in Figure 5. Consistent with our expectation of reduced double bond character upon ring opening, the rotational energy barrier using the new parameters is about 7 kcal/mol, much lower than the 19 kcal/mol obtained using ff99-based parameters. In addition, the new parameters adjust the relative energies of the minima at 0° and 180° by 2.7 kcal/mol. In ff99, these minima had the same values.

Energy Profiles for N7—C8 Bond Rotation

Since the barrier for rotation about the C5—N7 bond required modification, we also calculated the energy profile for rotation about the neighboring N7—C8 bond using a similar procedure as described for C5—N7. The results are shown in Table 2. The resulting parameters are provided in Table 3, along with those from standard ff99.

In this case the main energy barrier for the rotation around N7—C8 is the same in the new and original parameter sets (20 kcal/mol). A minor difference is that in the new parameter set the *cis* conformation of this dihedral angle is 4 kcal/mol less stable than *trans* conformation. However, this difference may not be noticeable during normal simulations because of the large height of the barrier separating these minima (20 kcal/mol). In our simulations of DNA in solution and in complex no transition between these conformations has been observed.

Results Using the New Parameters

The molecular mechanics energy of FapydG was calculated using standard Amber ff99 force field with these new torsional energy terms for rotation about C5—N7 and N7—C8. As shown in Figure 4, the resulting energy profiles are in much better agreement with the MP2 data, and the profiles for both *cis* and *trans* N7—C8 are reproduced with a single set of parameters.

Similar to the simulations described above using standard ff99, simulations of the *B. St.* Fpg/DNA complex containing FapydG were performed in explicit solvent using the new dihedral parameters. The starting structure for FapydG was obtained from the X-ray structure of *c*FapydG (PDB ID 1XC8), with a nonplanar, *cis* FapydG conformation. We analyzed the planarity of the FapydG as well as the interaction between FapydG and Tyr241. In Figure 6a, we show that a stable hydrogen bond is formed between the OH of Tyr241 and the phosphate O1P atom of FapydG, with an average distance of 2.7 6 0.2 Å. The distance between FapydG O8 and Tyr241 is much longer (Fig. 6a); visual analysis revealed that both FapydG and Tyr241 hydrogen bond to a bridging water molecule, although the water exchanges with bulk solvent during the simulation (Fig. 7). The water bridge between O8 of

FapydG and OH of Tyr was lost at the beginning of the simulation but reformed after ~1500 ps. After that point the distance between O8 of FapydG and OH of Tyr241 was stable at ~6 Å with fluctuations when the water again exchanged with the bulk at ~3000 ps. Figure 7 shows the overlap of the two snapshots from different time points in the MD simulation with the X-ray structure of the Fpg/cFapydG complex. Not only do FapydG and Tyr214 from our simulation neatly align with the X-ray conformation, but the relatively more mobile water molecules involved in the water bridge also appear at about the same position as the one in the X-ray structure, even though exchanges occurred. In the simulation using the standard ff99 dihedral parameters, FapydG strongly preferred a planar conformation (the dihedral angle C4—C5—N7—C8 is ~0°, Fig. 6), precluding the possibility of formation of this water-bridged interaction.

Figure 6c shows the dihedral angle of C4—C5—N7—C8 in FapydG during the simulation. In the simulation using the new parameters, a correlation is apparent between the formation of the water bridge and the value of this dihedral angle. When the water bridge was not stable (0–1500 ps), the dihedral angle of C4—C5—N7—C8 was closer to planar (−30°). After formation of the water bridge, (1500–2900 ps), this dihedral angle was highly nonplanar (~−100°), in good agreement with the crystal structure (−103°). This correlation suggests that the formation of the water bridge stabilizes the nonplanar conformation, since the energy minimum for the isolated *cis* FapydG occurs in the planar conformation (Fig. 4). Hence the energy penalty of the nonplanar conformation is balanced by the formation of the water bridged interaction. In the simulations using ff99 dihedral parameters, which overestimated the rotation energy barrier by 10 kcal/mol (Fig. 5), the dihedral penalty cannot be overcome by the water bridge.

We previously reported that E77 in B. st. Fpg has significant effects on the binding mode of 8-oxo-guanine.[18] Therefore, we also extended our simulation using the new parameter set with the E77S mutant of *B. st.* Fpg. The results are shown in Figure S2. The dihedral angle of C4—C5—N7—C8 was maintained at about 20° for about 1 ns. Then it switched to —40°, retaining that value for the remainder of the ~4 ns simulation. In thissimulation, there was no water bridge formation observed. Thus we conclude that the water bridge and significantly nonplanar FapydG conformation which seem important in lesion binding in *L. lactis* Fpg (PDB ID 1XC8) and *B. st.* Fpg (in our simulations, Fig. 6) may be absent in the majority of Fpg sequences that have Ser at this position. Therefore, the biological relevance of the highly nonplanar lesion conformation observed in the crystal structure remains unclear.

Conclusion

We performed quantum mechanical and molecular mechanical calculations, which confirmed that different molecular mechanics dihedral parameters are required for the opened ring of FapydG. This increases the flexibility of the dihedral angle C4— C5—N7—C8 through a reduction in the effective dihedral barrier by about 10 kcal/mol. When simulations were performed with standard ff99 parameters, we obtained a planar FapydG conformation, in disagreement with a crystal structure. The new parameters more faithfully reproduce both the positions of energy minima and the also the height of the barriers that are

obtained through *ab initio* calculations. When used in simulations of a FapydG-containing DNA duplex bound to the DNA glycosylase Fpg, the new parameters reproduced the nonplanar conformation for *c*FapydG observed in a crystal structure of the *L. lactis* Fpg/DNA complex. This conformation was observed to be stabilized through a water-bridged interaction with Tyr241 in *L. lactis* Fpg, which appears to counteract the intrinsic penalty for the nonplanar FapydG conformation. This balance between competing interactions was incorrect in ff99. The new parameters are expected to be a crucial component of future studies of the important FapydG lesion, which is particularly difficult to study using experimental synthesis techniques.

It is interesting to note that a previous simulation study using ff99 reported[16] a moderately nonplanar conformation for FapydG bound to *E. coli* Fpg. In this case, FapydG was in the *trans* conformation, which has a nonplanar conformation as the energy minimum with both standard ff99 and the new parameters. The extent of the nonplanar distortion reported in that work is substantially lower than observed in the *L. lactis* crystal structure; however, our simulations of the E77S *B. st.* Fpg mutant (corresponding to the *E. coli* sequence) also showed significantly more planar FapydG structures than we obtained in the presence of the acidic residue. Taken together, these studies suggest that the highly nonplanar *c*FapydG conformation observed in the crystal structure with *L. lactis* Fpg may not represent a general feature of FapydG recognition.

Acknowledgments

CS is a Cottrell Scholar of Research Corporation.

References

1. Frieberg, EC.; Walker, GC.; Siede, W.; Wood, RD.; Shultz, R.; Ellenberger, T. DNA Repair and Mutagenesis. Washington, DC: ASM; 2006.
2. Halliwell, B.; Gutteridge, JMC. Free Radicals in Biology and Medicine. Oxford: Oxford University Press; 1999.
3. Kasai H, Nishimura S. Nucleic Acids Res. 1984; 12:2137. [PubMed: 6701097]
4. Bjelland S, Seeberg E. Mutat Res. 2003; 531(1/2):37. [PubMed: 14637246]
5. Grollman AP, Moriya M. Trends Genet. 1993; 9(7):246. [PubMed: 8379000]
6. Pouget JP, Douki T, Richard MJ, Cadet J. Chem Res Toxicol. 2000; 13(7):541. [PubMed: 10898585]
7. Lindahl T. Br J Cancer. 1987; 56(2):91. [PubMed: 3311110]
8. Delaney MO, Greenberg MM. Chem Res Toxicol. 2002; 15(11):1460. [PubMed: 12437337]
9. Haraguchi K, Delaney MO, Wiederholt CJ, Sambandam A, Hantosi Z, Greenberg MM. J Am Chem Soc. 2002; 124(13):3263. [PubMed: 11916409]
10. Wiederholt CJ, Delaney MO, Pope MA, David SS, Greenberg MM. Biochemistry. 2003; 42(32): 9755. [PubMed: 12911318]
11. Patro JN, Haraguchi K, Delaney MO, Greenberg MM. Biochemistry. 2004; 43(42):13397. [PubMed: 15491146]
12. Coste F, Ober M, Carell T, Boiteux S, Zelwer C, Castaing B. J Biol Chem. 2004; 279(42):44074. [PubMed: 15249553]
13. Ober M, Linne U, Gierlich J, Carell T. Angew Chem Int Ed Engl. 2003; 42(40):4947. [PubMed: 14579447]

14. Ober M, Muller H, Pieck C, Gierlich J, Carell T. J Am Chem Soc. 2005; 127(51):18143. [PubMed: 16366567]
15. Fromme JC, Verdine GL. J Biol Chemi. 2003; 278(51):51543.
16. Perlow-Poehnelt RA, Zharkov DO, Grollman AP, Broyde S. Biochemistry. 2004; 43(51):16092. [PubMed: 15610004]
17. Wang JM, Cieplak P, Kollman PA. J Comput Chem. 2000; 21(12):1049.
18. Song K, Hornak V, Santos CD, Grollman AP, Simmerling C. Biochemistry. 2006; 45(36):10886. [PubMed: 16953574]
19. Cieplak P, Cornell WD, Bayly C, Kollman PA. J Comput Chem. 1995; 16(11):1357.
20. Gaussian03, RC.; Frisch, MJ.; Trucks, GW.; Schlegel, HB.; Scuseria, GE.; Robb, MA.; Cheeseman, JR.; Montgomery, JA., Jr; Vreven, T.; Kudin, KN.; Burant, JC.; Millam, JM.; Iyengar, SS.; Tomasi, J.; Barone, V.; Mennucci, B.; Cossi, M.; Scalmani, G.; Rega, N.; Petersson, GA.; Nakatsuji, H.; Hada, M.; Ehara, M.; Toyota, K.; Fukuda, R.; Hasegawa, J.; Ishida, M.; Nakajima, T.; Honda, Y.; Kitao, O.; Nakai, H.; Klene, M.; Li, X.; Knox, JE.; Hratchian, HP.; Cross, JB.; Bakken, V.; Adamo, C.; Jaramillo, J.; Gomperts, R.; Stratmann, RE.; Yazyev, O.; Austin, AJ.; Cammi, R.; Pomelli, C.; Ochterski, JW.; Ayala, PY.; Morokuma, K.; Voth, GA.; Salvador, P.; Dannenberg, JJ.; Zakrzewski, VG.; Dapprich, S.; Daniels, AD.; Strain, MC.; Farkas, O.; Malick, DK.; Rabuck, AD.; Raghavachari, K.; Foresman, JB.; Ortiz, JV.; Cui, Q.; Baboul, AG.; Clifford, S.; Cioslowski, J.; Stefanov, BB.; Liu, G.; Liashenko, A.; Piskorz, P.; Komaromi, I.; Martin, RL.; Fox, DJ.; Keith, T.; Al-Laham, MA.; Peng, CY.; Nanayakkara, A.; Challacombe, M.; Gill, PMW.; Johnson, B.; Chen, W.; Wong, MW.; Gonzalez, C.; Pople, JA. Wallingford CT: Gaussian, Inc.; 2004.
21. Cornell WD, Cieplak P, Bayly CI, Kollman PA. J Am Chem Soc. 1993; 115(21):9620.
22. Case DA, Cheatham TE, Darden T, Gohlke H, Luo R, Merz KM, Onufriev A, Simmerling C, Wang B, Woods RJ. J Comput Chem. 2005; 26(16):1668. [PubMed: 16200636]
23. Jorgensen WL, Chandrasekhar J, Madura JD, Impey RW, Klein ML. J Chem Phys. 1983; 79(2): 926.
24. Zaika EI, Perlow RA, Matz E, Broyde S, Gilboa R, Grollman AP, Zharkov DO. J Biol Chem. 2004; 279(6):4849. [PubMed: 14607836]
25. Ryckaert JP, Ciccotti G, Berendsen HJC. J Comput Phys. 1977; 23(3):327.
26. Berendsen HJC, Postma JPM, Vangunsteren WF, Dinola A, Haak JR. J Chem Phys. 1984; 81(8): 3684. Molecular Mechanics Parameters for the FapydG DNA lesion 23.

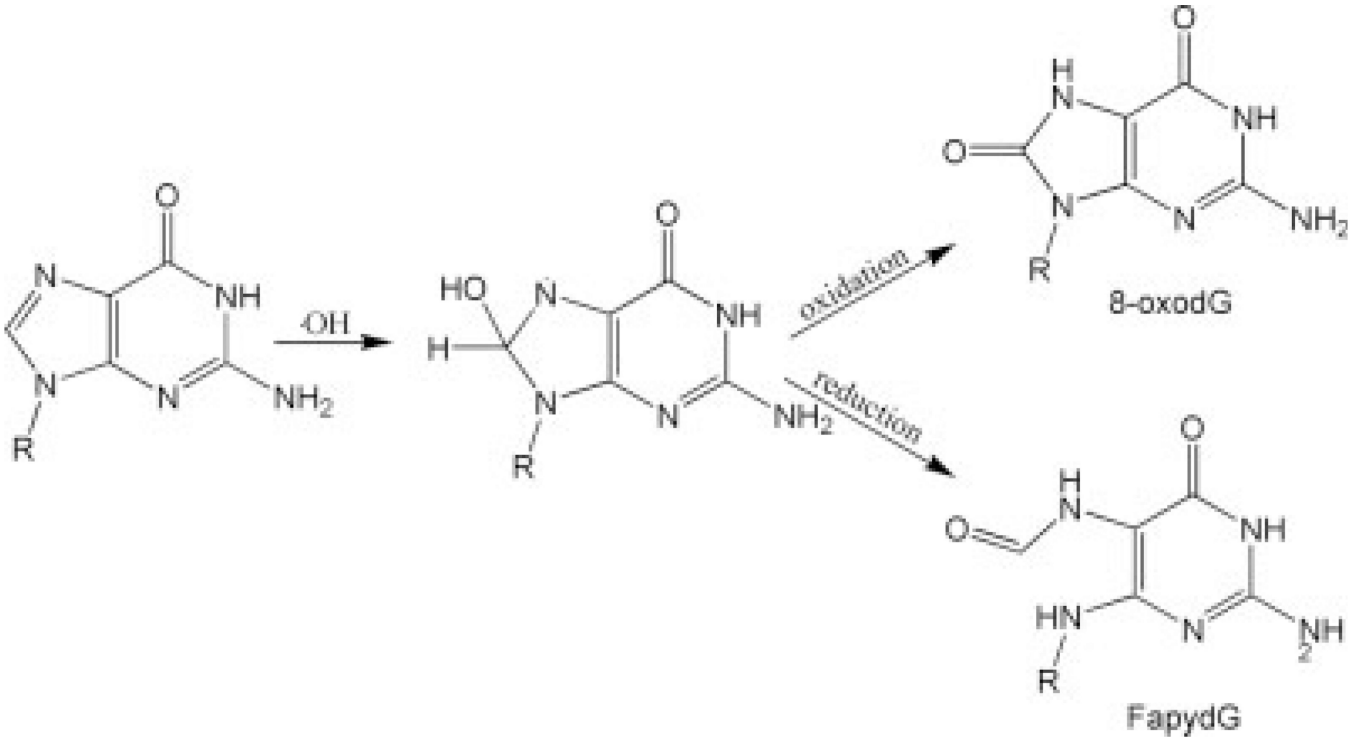

Figure 1.
The formation of 8-oxodG and FapydG by hydroxyl radicals. Note the loss of the imidazole ring in FapydG that is retained in 8-oxodG.

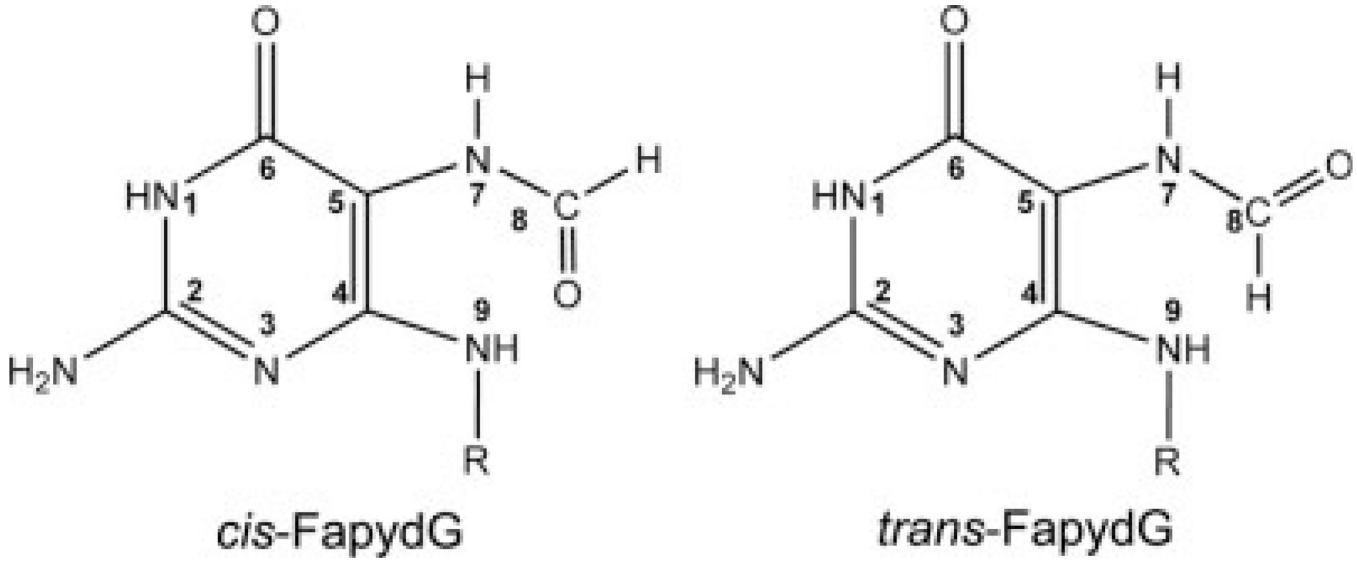

Figure 2.

The structures of two isomers for FapydG. In cis-FapydG the N7—C8 bond is in the cis configuration, while in trans-FapydG the N7—C8 bond is *trans*.

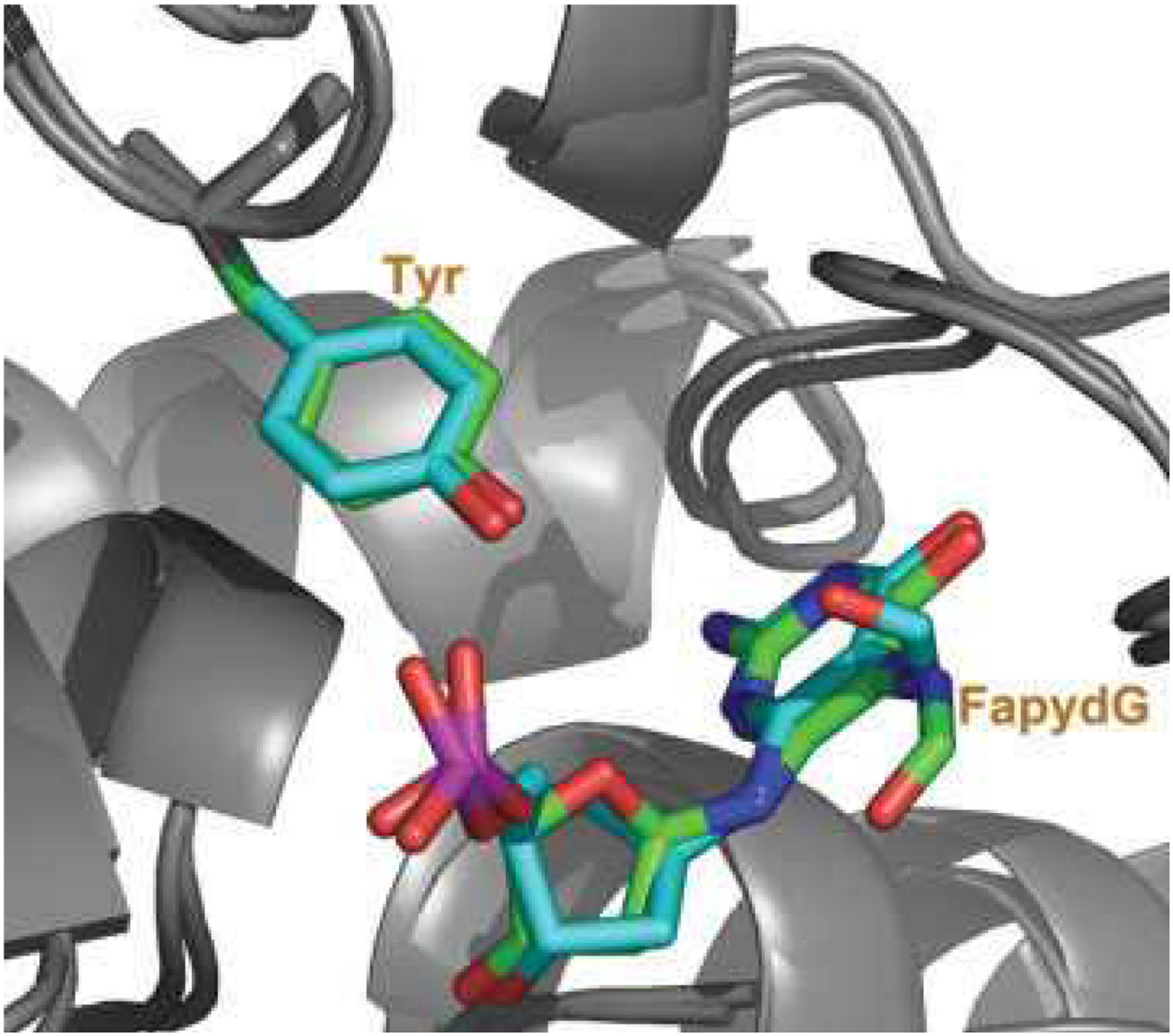

Figure 3.

The conformation of *L. lactis* Fpg bound to *c*FapydG containing DNA in the X-ray structure (pdb ID 1XC8, carbon atoms shown in cyan) and the simulated conformation of *B. st.* Fpg bound to FapydG containing DNA using standard ff99-based parameters (carbon atoms shown in green). Heavy atoms are shown only for FapydG and Tyr238. Although the FapydG simulation was initiated with the crystal structure, the nonplanar conformation of *c*FapydG was not retained when lusing standard ff99 parameters.

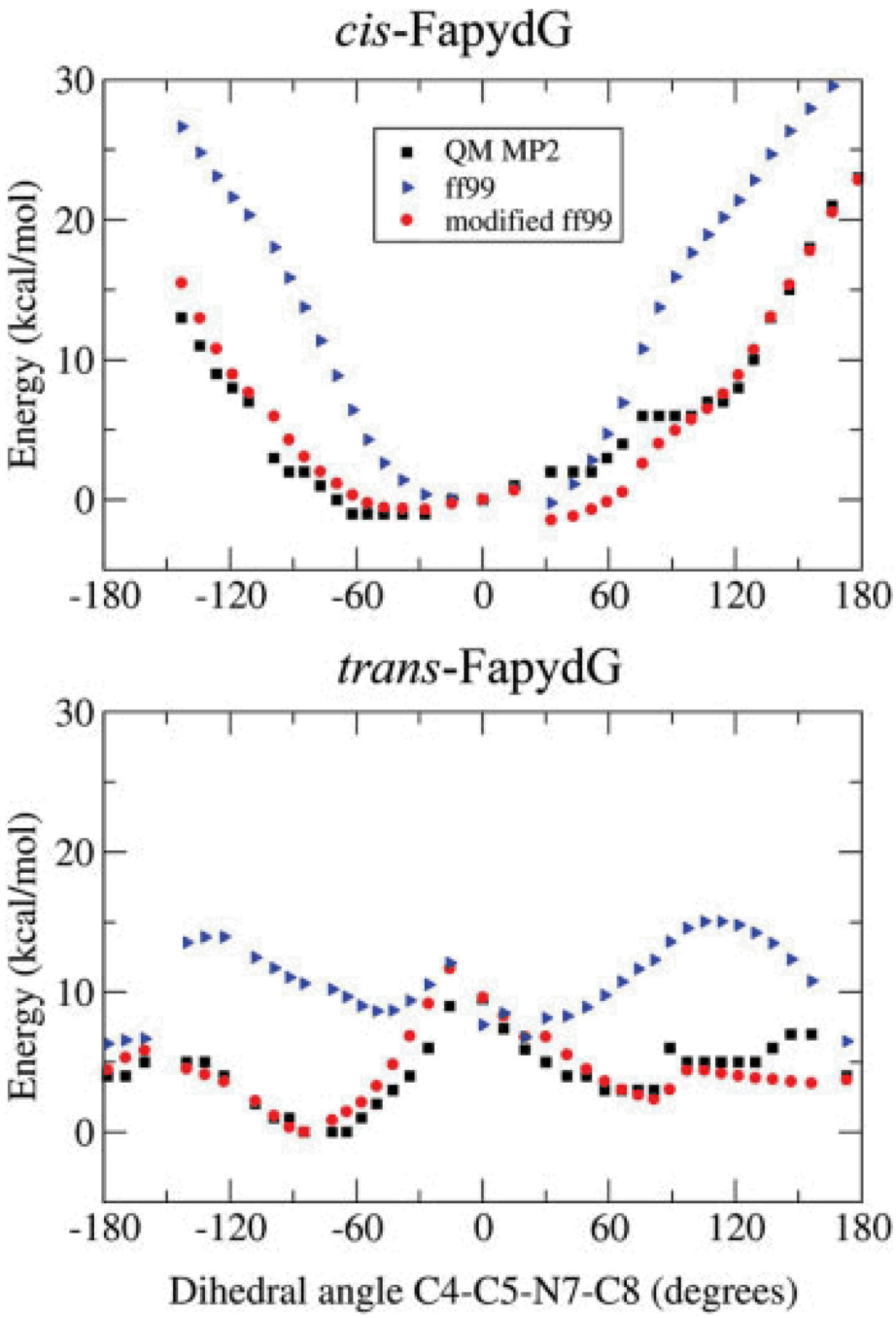

Figure 4.

Total energies as a function of C4—C5—N7—C8 dihedral angle, for *cis* and *trans* FapydG. The energies were obtained using *ab initio* calculations (black square), molecular mechanics with torsion parameters obtained from ff99 (blue triangles) and molecular mechanics with ff99 and our modified torsion energy terms (red circle). The new profiles are in much better agreement with the *ab initio* data than those obtained using ff99.

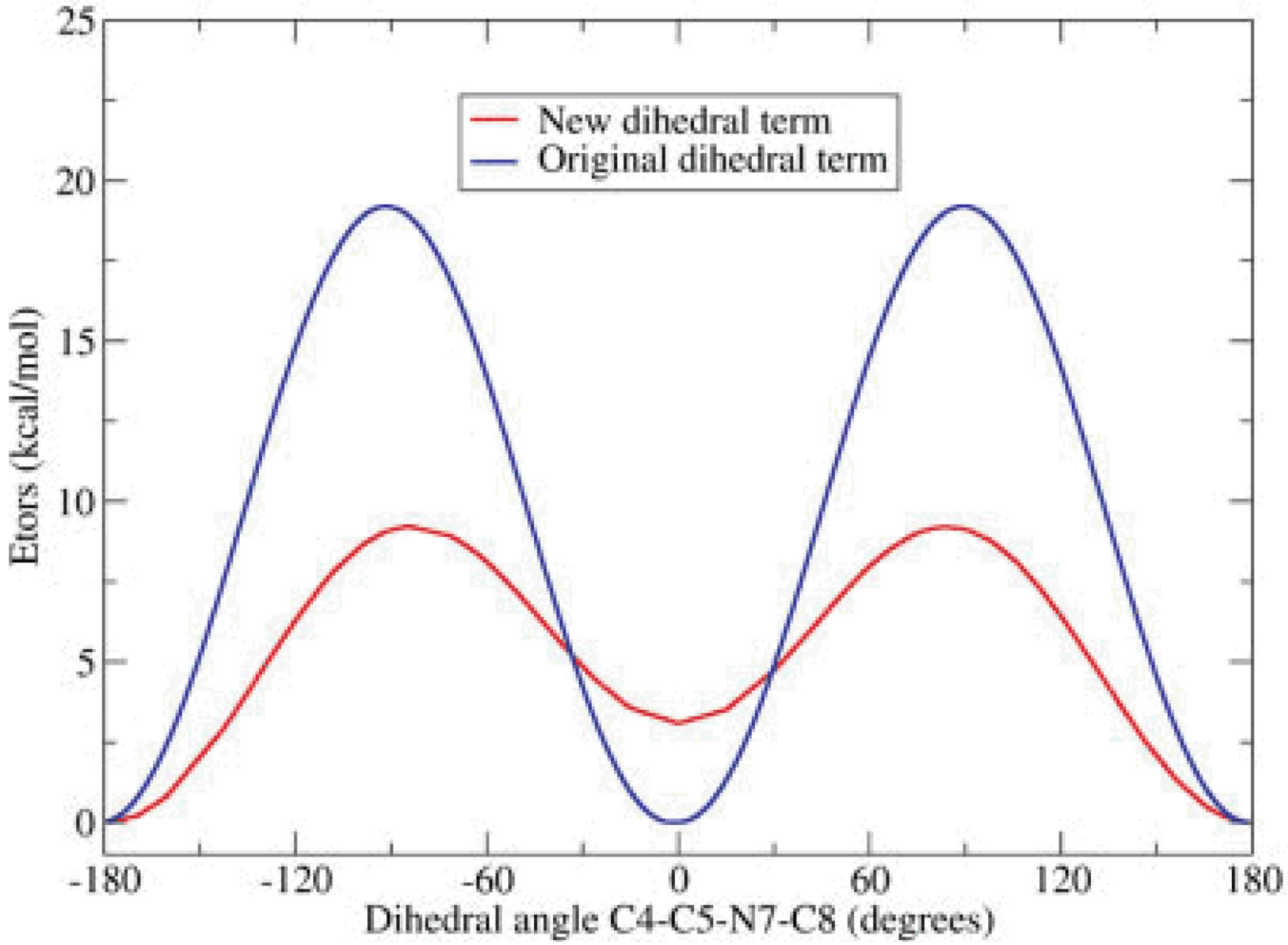

Figure 5.

Dihedral angle energies for rotation about the C5—N7 bond. Only the dihedral energy [eq. (1)] is shown. The blue line represents standard ff99, and the red line represents the new parameters obtained through fitting to the QM energies.

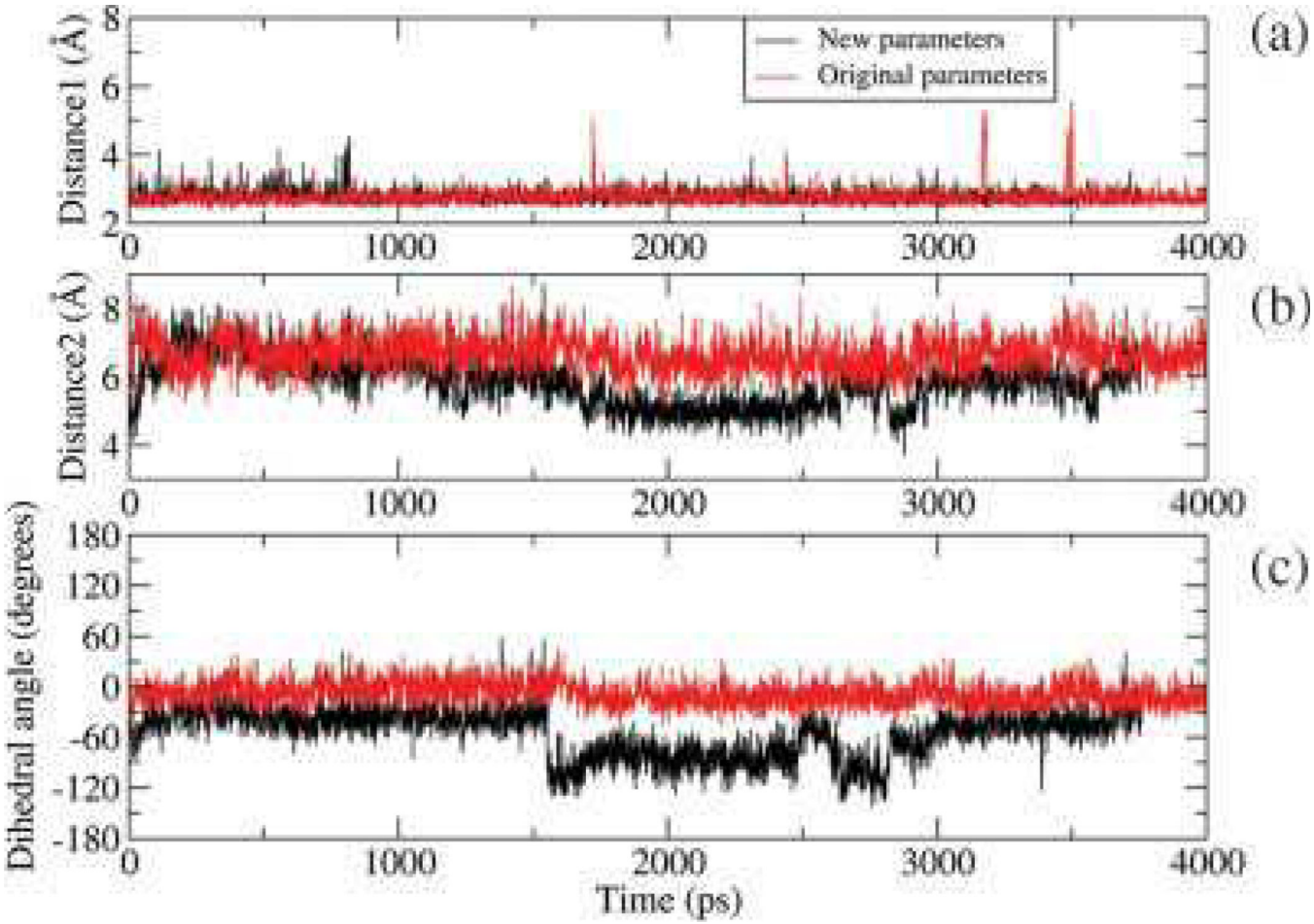

Figure 6.

Dihedral angles and distances in the *B. st*. Fpg/FapydG simulation with new (black) and original (red) ff99 dihedral parameters. Distance 1 is the distance of O1P of FapydG to OH of Tyr238, distance 2 is the distance of O8 of FapydG to OH of Tyr238, and dihedral angle is the C4—C5—N7—C8 dihedral angle. In the crystal structure these values are 2.59 Å, 5.08 Å, and -103.74°, respectively.

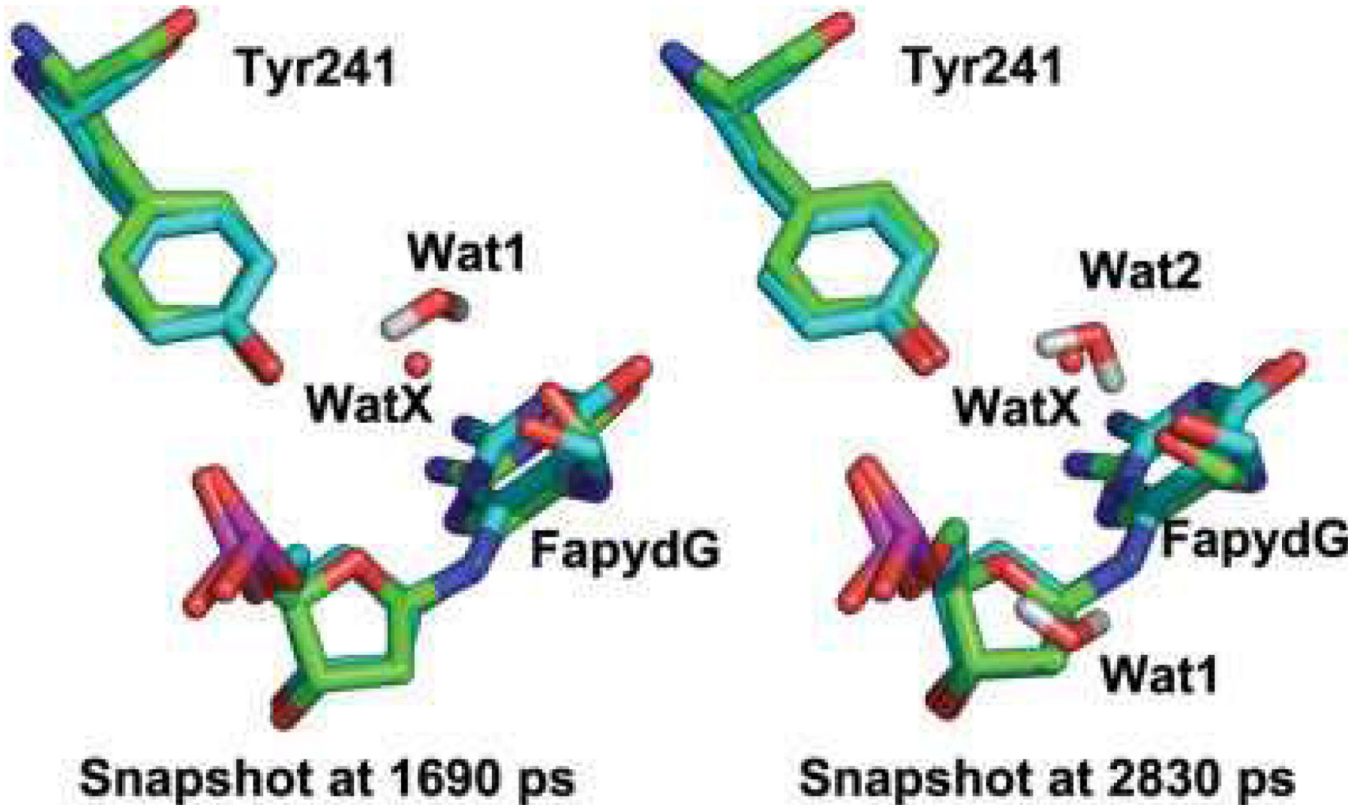

Figure 7.

Two snapshots from *B. st*. Fpg/FapydG simulation (carbons in green) overlapped on the X-ray structure of *c*FapydG (carbons in cyan). Two MD snapshots are shown (1690 ps and 2830 ps), in which two different water molecules (labeled Wat1 and Wat2) play the role in bridging the interaction between FapydG and Tyr241. The FapydG conformation and position of the bridging water molecules are in good agreement with the crystal structure (with water labeled WatX).

Table 1

New and ff99-Based Torsion Parameters for Rotation About the C5—N7 Bond, Using the Function Provided in Eq. (1).

	V_1 (kcal/mol)	n_1	γ_1 (degrees)	V_2 (kcal/mol)	n_2	γ_2 (degrees)
ff99	9.6	2	180	-	-	-
New values	3.52	2	180	1.36	1	0

The dihedral angle is represented by the atoms C4—C5—N7—C8.

Table 2

Energies of Four FapydG Conformations With Different C5—N7—C8—O8 Dihedral Angle and *cis* C4—C5—N7—C8.

Dehedral angle (degrees)	Energy: MP2 (kcal/mol)	Energy: MM (ff99) (kcal/mol)	Energy: MM (new) (kcal/mol)
0	−2	−6.2	−3.2
90	19	14.3	17.3
180	0	0	0.0
270	29	28.3	29.8